ASSESSMENT OF MANGROVE EXTENT EXTRACTION ACCURACY OF THRESHOLD SEGMENTATION-BASED INDICES USING SENTINEL IMAGERY

C. D. C. Zablan [1], A. C. Blanco [1 2 3], K. Nadaoka [4], K. P. Martinez [1], A. B. Baloloy [1]

[1] Department of Geodetic Engineering, University of the Philippines Diliman, Quezon City 1101, Philippines
[2] Training Center for Applied Geodesy and Photogrammetry, University of the Philippines, Diliman, Quezon City 1101, Philippines
[3] Philippine Space Agency, Diliman, Quezon City 1101, Philippines
[4] Department of Transdisciplinary Science and Engineering, Tokyo Institute of Technology, Tokyo, Japan
cczablan1@up.edu.ph

Commission IV, WG7

KEY WORDS: Mangrove index, Sentinel-2, Sentinel-1, Google Earth Engine, Mangrove Extent

ABSTRACT:

Mangroves have been protecting coastlines, nourishing wildlife, and capturing carbon for climate regulation. The decline of mangroves calls for action to rapidly and accurately monitor them. Remote Sensing makes it possible to remotely monitor mangroves from images captured from space. Sentinel-1 and Sentinel-2 are examples of remote sensing satellites and there is extensive research on their land cover mapping capabilities, including mangrove mapping. While machine learning is a popular methodology for mangrove mapping (e.g., the use of Random Forest) there exist simpler techniques, i.e., utilizing threshold segmentation-based indices that only use a formula and a specific threshold to extract mangrove extents from satellite imagery (mostly Sentinel imagery). This study compared the products and the accuracy of different threshold segmentation-based mangrove mapping indices in four study areas in the Philippines and one in Indonesia. Results showed that the Mangrove Vegetation Index (MVI), Automatic Mangrove Map and Index (AMMI), and the Optical and SAR images Combined Mangrove Index (OSCMI) subindex SWIRB (full name of this subindex here) were the superior indices with overall accuracies (OA) greater than 80% in all study areas and reaching a maximum of 90%, 91% and 96%, respectively. By McNemar’s test showed that their results have insignificant differences. MVI, SWIRB, and AMMI only used Sentinel-2 optical imagery, which means the addition of Sentinel-1 SAR imagery was unnecessary. Since the validation data is a product of machine-learning classification, this shows that using threshold segmentation-based indices is promising as it is simpler, faster, and requires little skill compared to using classification techniques.

1. INTRODUCTION

Mangroves are coastal trees and shrubs that provide coastline support from surges, waves, currents, and tides (National Oceanic and Atmospheric Administration [NOAA], 2021). The root system of mangroves is home to marine organisms (NOAA, 2021). These vegetation are also part of the blue carbon ecosystem as they capture and hold carbon for thousands of years faster than other forests, which is helpful against climate change (NOAA, 2013).

However, Goldberg (2020) found that Earth lost 2.1% of mangrove area between 2000 and 2016, at an annual rate of 0.13%. Mangroves are decreasing due to land conversion to agriculture and aquaculture (Gevaña et al., 2019; Goldberg, 2020). The decrease of these forests may make countries that benefit from them more vulnerable to disasters, loss of biodiversity, and climate change. Thus, accurate and rapid monitoring of mangrove extent may prevent further deforestation of the mangroves. Remote Sensing makes this possible with satellite imagery. It is less expensive as free satellite imagery is available, e.g., Sentinel and Landsat imagery. Images captured years ago are also stored, allowing temporal analysis.

To aid in mangrove extent extraction, researchers have developed indices that aim to improve the separability of mangroves from other land cover classes (Table 1). Many researchers used machine learning algorithms to accurately classify mangrove pixels (Goldberg, 2020; Kamal, 2020; Mondal et al., 2019; Pham et al., 2021). Proponents of some mangrove mapping indices claim that fusing or using their product image and applying machine-learning algorithms improves classification accuracy (Shi et al., 2016; Kumar et al., 2017; Gupta et al., 2018; Xia et al., 2018; Jia et al., 2018). Xue and Qian (2022) recently developed the Generalized Composite Mangrove Index for Mapping Mangroves (GCMI). The index is built from several other indices and is imported to the Random Forest (RF) classifier. Its results were compared to other indices, including a threshold-segmentation based mangrove index, i.e., the Mangrove Vegetation Index (MVI) (Baloloy et al., 2020). CGMI has the highest overall accuracy, but it differs only by around 2% from MVI. Since machine learning algorithms like the RF can be computationally expensive, the slight extraction enhancement may not justify the significant additional efforts. Thus, researchers have developed threshold segmentation-based mangrove mapping indices that only require a specific threshold to separate it from non-mangroves (Huang et al., 2022; Baloloy et al., 2020; Jia et al., 2018; Suyarso, 2022; Zhang & Tian., 2013).

Optical and SAR images Combined Mangrove Index (OSCMI) is one of the latest threshold segmentation-based mangrove extracting indices (Huang et al., 2022). The proponents showed that the addition of synthetic aperture radar (SAR) imagery produced higher accuracy than MVI. Thus, this study compared the accuracy of existing threshold segmentation-based mangrove extraction indices with several study sites and used a machine-learning algorithm to validate the results. This study will also include Automatic Mangrove Map and Index (AMMI) by Suyarso (2022), which markets itself as an index that captures and traces mangroves extent, and simultaneously displays the relative index of mangroves canopy density. Furthermore, Mangrove Forest Index (MFI), was also included even though it is primarily for separating submerged mangroves from water to also test its capability in general mangrove extraction. The

[1]* Corresponding author

findings of the study will provide mangrove mappers insight on what index is best to use and some guidelines on the specific threshold values used in separating mangroves from non-mangrove vegetation.

Index	Proponents	Data Used
Classification algorithm-based		
Normalized Difference Mangrove Index (NDMI)	Shi et al. (2016)	Landsat
Mangrove Probability Vegetation Index (MPVI)	Kumar et al. (2017)	EO-1 Hyperion
Combine Mangrove Recognition Index (CMRI)	Gupta et al. (2018)	Landsat-8
Submerged Mangrove Recognition Index (SMRI)	Xia et al. (2018)	GF-1
Mangrove Forest Index (MFI)	Jia et al. (2018)	Sentinel-2
Generalized Composite Mangrove Index (GCMI)	Xue & Qian (2022)	Sentinel-2
Threshold segmentation-based		
Mangrove Recognition Index (MRI)	Zhang and Tian (2013)	Landsat TM
Mangrove Forest Index (MFI)	Jia et al. (2018)	Sentinel-2
Mangrove Vegetation Index (MVI)	Baloloy et al. (2020)	Landsat or Sentinel-2
Automatic Mangrove Map and Index (AMMI)	Suyarso (2022)	Landsat 5,7, 8 or Sentinel-2
Optical and SAR images Combined Mangrove Index (OSCMI)	Huang et al. (2022)	Sentinel-1 and Sentinel -2

Table 1. Indices for Mangrove Mapping

1.1 Study Area

In Southeast Asia and Asia-Pacific, the Philippines is considered one of the primary hotspots for mangrove deforestation and Indonesia is secondary (Gandhi & Jones, 2019). It is important for these countries to monitor mangrove covers to reduce the deforestation rate. Palawan, Surigao del Norte and Sur, and Tawi-Tawi are four of the top provinces in the Philippines with largest mangrove cover at percentages of total national area 22.2%, 6.8%, and 4.4%, respectively (Viray-Mendoza, 2017). Puerto Princesa City and Busuanga of Palawan, Siargao Island of Surigao del Norte, and Languyan, Bongao, Panglima Sugala, Sapa-Sapa, Tandubas, and South Ubian of Tawi-Tawi are selected as study areas of this research. To test the indices in a different country, the researchers chose Karimunjawa and Kemujan Islands, Indonesia as additional study areas. The researchers chose subsites, represented by the footprints of the images, for validation (Figure 1).

Figure 1. Google Earth maps of selected study areas with PlanetScope true color image and its footprint overlaid. (A) Puerto Princesa City, Palawan, Philippines; (B) Busuanga, Palawan, Philippines; (C) Siargao Island, Surigao del Norte, Philippines; (D) Province of Tawi-Tawi, Philippines; (E) Karimunjawa-Kemujan Islands, Indonesia.

2. DATA AND METHODS

The workflow of this study is presented in Figure 2. The study used three types of satellite imagery. Sentinel-1 and Sentinel-2 are free and open access imagery, while the commercial PlanetScope Imagery at a higher resolution was provided by Planet for free for this study. The PlanetScope imagery was classified to serve as the validation data for the accuracy assessment of the threshold segmentation-based indices. Before using it as validation data, it also underwent accuracy assessment using several reference data. Since MVI and OSCMI (including subindices) required thresholding to produce the optimal results, it was also applied to other indices to see the variability of the indices, especially in different study areas.

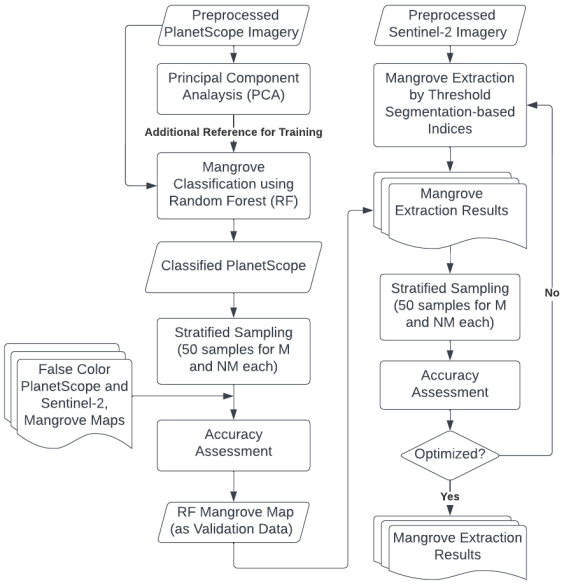

Figure 2. General workflow of the study

2.1 Satellite data and pre-processing

Google Earth Engine (GEE)—a cloud-computing platform that houses satellite image collections and allows processing and analysis of large geospatial datasets—was used throughout this study (Gorelick et al., 2017).

Sentinel-2 MSI: MultiSpectral Instrument, Level-2A image collection provides orthorectified and atmospherically corrected surface reflectance data. Temporal median reduction is applied to all images of Puerto Princesa in this collection throughout 2020, with a cloud cover of less than 20%. However, the cloud cover requirement is extended to 30% for Siargao as half of the island does not have Sentinel-2 imagery meeting the 20% requirement throughout the year.

Sentinel-1 SAR GRD: C-band Synthetic Aperture Radar Ground Range Detected, log scaling image collection provides calibrated and ortho-corrected product with GRD border noise and thermal noise removed. Temporal median reduction is again applied to all Interferometric Wide Swath (IWS) images of Puerto Princesa in this collection throughout 2020. The image composite is then reprojected to the Sentinel-2's image composite's map projection.

Mangroves are coastal vegetation where elevations are relatively low. Thus, a vegetation mask and an elevation mask of values less than 35 meters were applied to Sentinel-2 and Sentinel-1 using Sentinel-2 Level 2A Scene Classification Layer (SCL) and NASA SRTM Digital Elevation, respectively, to all image collections used in the study.

PlanetScope imagery for each study site in 2020 with low cloud cover was utilized and classified for accuracy assessment purposes. The images have eight (8) bands and are in surface reflectance that is harmonized to Sentinel-2 values. However, Tawi-Tawi does not have an available 8-band image for that year. The researchers settled with a 4-band image, instead. Clear masking was then applied to remove the cloud, cloud shadow, haze, and snow.

All images are clipped to each study area's administrative boundaries.

2.2 Threshold segmentation-based mangrove indices

This study used mangrove extracting indices that only require a specific threshold to separate mangroves from other land cover classes and do not require tidal data. These indices are Mangrove Recognition Index (MRI), Mangrove Forest Index (MFI), Mangrove Vegetation Index (MVI), Optical and SAR images Combined Mangrove Index (OSCMI), and Automatic Mangrove Map and Index.

However, Mangrove Recognition Index (MRI) was developed using multi-temporal Landsat TM images with different tide levels (Zhang & Tian, 2013). The index requires tidal data which is counterproductive to the goal of rapid mangrove mapping. Hence, it was excluded from this study.

To aid in optimizing threshold values for mangrove extraction, stratified sampling of the classified validation image with 50 samples each for mangroves and non-mangroves for each study area, following Olofsson et al. (2014). The corresponding threshold segmentation-based index values were then extracted from those samples. The data was then visualized through box plots to show the distribution of index values for mangroves and non-mangroves.

2.2.1 Mangrove Forest Index (MFI)

MFI is the first index to address the mangrove mapping limitation of needing multi-tide imagery. It was developed to separate submerged mangrove forests from water by using red-edge bands using Sentinel-2 imagery (Jia et al., 2019).

$$MFI = [(\rho_{\lambda 1} - \rho_{B\lambda 2}) + (\rho_{\lambda 2} - \rho_{B\lambda 2}) + (\rho_{\lambda 3} - \rho_{B\lambda 3}) + (\rho_{\lambda 4} - \rho_{B\lambda 4}) \quad (1)$$

where the $\rho_{\lambda i}$ is the reflectance of the band center of λ, and i ranged from 1 to 4; λ1, λ2, λ3, λ4 represent the center wavelengths at 705, 740, 783 and 865 nm, respectively. $\rho_{B\lambda i}$ is the baseline reflectance in λi. ρ_{665} and ρ_{2190} are the reflectance of band 4 (centered at 665 nm) and 12 (centered at 2190 nm), respectively.

$$\rho_{B\lambda i} = \rho_{2190} + (\rho_{665} - \rho_{2190}) \times (2190 - \lambda i)/(2190 - 665) \quad (2)$$

The Sentinel-2 bands used in this index have different spatial resolutions. When performing analysis in GEE, the bands ingested are automatically resampled to the band with the highest resolution.

The minimum threshold for submerged mangrove mapping of MFI is 0 (Jia et al., 2019). However, the proponents did not examine mangrove extraction from other vegetation types.

2.2.2 Mangrove Vegetation Index (MVI)

MVI was developed to separate different land cover and land use classes from mangroves using single-tide imagery. It was formulated from the common usage of NIR and SWIR in several mangrove mapping indices. Both Sentinel-2 and Landsat-8 imagery are tested with MVI. The recommended range threshold is 4.5 to 16.5 (Baloloy, 2020).

$$MVI = \frac{NIR - Green}{SWIR1 - Green} \tag{3}$$

NIR, Green, and SWIR1 are the reflectances for bands 8, 3, and 11, respectively for Sentinel-2. For Landsat-8, they are bands 5, 3, and 6, respectively.

However, a recent assessment of the index by Neri et al. (2021) found that misclassification occurred in fishponds, croplands near mangrove sites, and areas in or near coastal regions with palm trees due to the similarity of spectral signatures with other vegetation in these areas. Thus, the optimal threshold for a large site may not be the same for its subsites (Neri et al., 2021).

2.2.3 Automatic Mangrove Map and Index (AMMI)

Suyarso (2022) developed a mangrove vegetation index that simultaneously extracts mangroves and computes canopy density precisely using optical satellite imagery, e.g., Sentinel-2 and Landsat-5, Landsat-7, and Landsat-8. The algorithm is the product of two equations. The first equation should separate the land and vegetation from water features. The second equation should map the extent of mangroves and display the canopy density. The proponent did not provide a threshold range but from his results, it was between 5 to 10.

$$AMMI = \frac{NIR - Red}{Red + SWIR1} \cdot \frac{NIR - SWIR1}{SWIR1 - 0.65 * Red} \tag{4}$$

NIR, Red, and SWIR1 are the reflectances for bands 8, 4, and 11, respectively for Sentinel-2. For Landsat 5 and 7, they are bands 4, 3, and 5, respectively. For Landsat 8, they are bands 5, 4, and 6, respectively.

2.2.4 Optical and SAR images Combined Mangrove Index (OSCMI)

Other than the two problems addressed by MFI and MVI, Huang et al. (2022) consider the vulnerability of optical images to clouds and fog as another problem in mangrove mapping. Hence, they introduced Synthetic Aperture Radar (SAR) imagery to solve this problem. This index can be computed by fusing SAR and optical imagery, i.e., Sentinel-1 and Sentinel-2 imagery. The formula is as follows:

$$OSCMI = \frac{WI}{NIRB + SWIRB + VV} \tag{5}$$

where WI is the sum of NDWI and MNDWI; NIRB is the sum of the reflectance of Sentinel-2 B6, B7, B8 and B8A; SWIRB is the sum of the reflectance of Sentinel-2 B11 and B12; VV is the backscatter coefficient of Sentinel-1 VV polarization mode (Huang et al., 2022). WI, NIRB, and SWIRB are not acronyms.

$$NDWI = \frac{Green - NIR}{Green + NIR} \tag{6}$$

$$MNDWI = \frac{Green - SWIR1}{Green + SWIR1} \tag{7}$$

Green, NIR, and SWIR1 are the reflectances for bands 3, 8, and 11, respectively for Sentinel-2. For Landsat-8, they are bands 3, 5, and 6, respectively.

OSCMI and its subindices WI, NIRB, and SWIRB were found to be more accurate than MVI in distinguishing mangrove from other vegetation (Huang et al., 2022). The threshold ranges from 0.04 to 0.07, -0.50 to -0.30, 0.95 to 1.10, and 0.15 to 0.20 for OSCMI, WI, NIRB, and SWIRB, respectively (Huang et al., 2022). However, its reliance on optical imagery does not solve the cloud and fog cover problem.

2.3 Accuracy Assessment

PlanetScope images captured in 2020 were classified into two classes, i.e., Mangroves and Non-Mangroves. The products were used for the accuracy assessment and comparison of the selected mangrove indices in this study.

Principal Component Analysis (PCA) reduces spectral information dimensionality by a linear transformation of the variation in a multiband image into a set of uncorrelated image bands (L3Harris, n.d.). The technique helps in visualizing patterns in a dataset (Powell, n.d.). Additionally, PCA is found to improve the classification process and results in Land Use Land Cover Mapping (LULC) compared to using the original dataset applied with mangrove as the interpretation error is minimized with better visualization of patterns (Abdu, 2019). The same was observed with mangrove differentiation from other vegetation (Green, 1998). Therefore, PCA was applied to the pre-processed PlanetScope images. The resulting Principal Component (PC) bands with high variance were selected as a guide in training the algorithm.

Different classification algorithms were compared in mangrove cover change monitoring and found that Random Forest (RF) machine learning algorithm performed the best (Elmahdy et al., 2020; Toosi et al., 2019). Thus, RF was utilized in this study to classify the PlanetScope images.

Stratified random sampling was employed for the validation of the classified PlanetScope images with 50 samples each for mangroves and non-mangroves classes. Sentinel-2 and PlanetScope False Color Combinations, and mangrove maps from previous studies were used as references. Accuracy assessment was performed. The metrics for accuracy used in this study are producer's accuracy (PA), user's accuracy (UA), overall accuracy (OA), and Kappa coefficient (κ).

To assess the mangrove extraction of the threshold segmentation-based indices, their image results and the classified PlanetScope image were concatenated into one multiband image. Stratified random sampling was employed again with 50 samples per class of the classified PlanetScope images. Accuracy assessment was then repeatedly performed to optimize the quality of the mangrove extracting indices with the classified PlanetScope image as reference.

McNemar's test is a statistical test for comparing two classification methods. It follows a chi-square distribution with one degree of freedom (Raschka, 2018):

$$\chi^2 = \frac{(B-C)^2}{B+C} \quad (8)$$

Where B is the number of misclassified samples from index 1 but classified correctly by index 2. Meanwhile, C is the number of misclassified samples from index 2 but classified correctly by index 1.

The p-value is computed and compared to the set significance level, i.e., 0.05. The null hypothesis is index 1 and index 2 produce statistically similar results. We reject the null hypothesis if the p-value exceeds the set significance level.

3. RESULTS AND DISCUSSION

3.1 Random Forest (RF) Mangrove Extraction

Table 2 shows the accuracy assessment results of the classified PlanetScope images using RF classifier. The metric values are greater than 80% (or 0.8 κ) in most study areas. The good results make them a valid reference for the accuracy assessment and thresholding of the indices.

Metric	Puerto Princesa City, Palawan, Philippines		Busuanga, Palawan, Philippines		Siargao, Surigao del Norte, Philippines		Tawi-Tawi Province, Philippines		Karimunjawa-Kemujan Islands, Indonesia	
OA (%)	**94.00**		**92.00**		**91.00**		**89.00**		**96.00**	
κ	0.88		0.84		0.82		0.78		0.92	
	NM	M	NM	M	NM	M	NM	M	NM	M
UA (%)	**92.00**	**96.00**	**96.00**	**88.00**	**92.00**	**90.00**	**80.00**	**98.00**	**94**	**98**
PA (%)	**95.83**	**92.31**	**88.89**	**95.65**	**90.20**	**91.84**	**97.56**	**83.05**	**97.92**	**94.23**

Table 2. Accuracy Assessment Results of Random Forest (RF) Classified PlanetScope Images.

Figure 4 provides insights into the separability of mangroves and non-mangroves. In Huang et al (2022), MVI showed poor separability from non-mangrove samples, unlike OSCMI and its subindices. However, in this study, it can be observed that MVI showed good and consistent separability in the five study areas. Meanwhile, OSCMI and its subindices, excluding SWIRB, showed poor to fair separability. Like MVI, SWIRB and AMMI showed good separability with the interquartile range (IQR) (or the boxes) of each class having separate values. Despite that, all indices have intersecting mangrove and non-mangrove index values, as seen in the box plots' whiskers. This result is different to the study of Baloloy et al. (2020) which showed no intersection between mangroves' and non-mangroves' MVI values. While possibly minimal for MVI, SWIRB, and AMMI, it can still affect the accuracy of the extraction.

This study agrees with Huang et al. (2022) that box plots are not enough to assess the reliability of these mangrove indices. However, they helped optimize the index threshold for the best extraction of mangroves. Table 3 shows each index's optimized extraction threshold and accuracy for every study area. Only SWIRB had an optimized threshold that was consistently within the recommendation of the proponents, except in Puerto Princesa with a slight difference. This may indicate that, like in Neri et al. (2021), the other indices' optimal mangrove extracting threshold may differ per location.

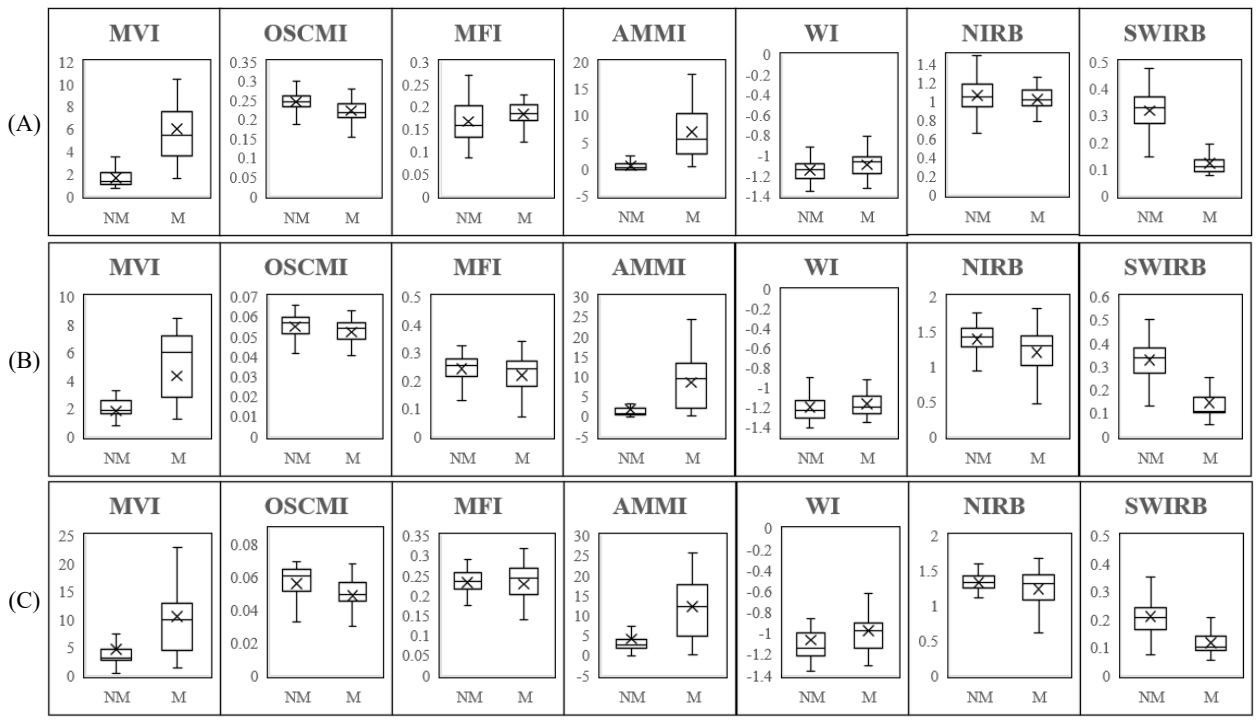

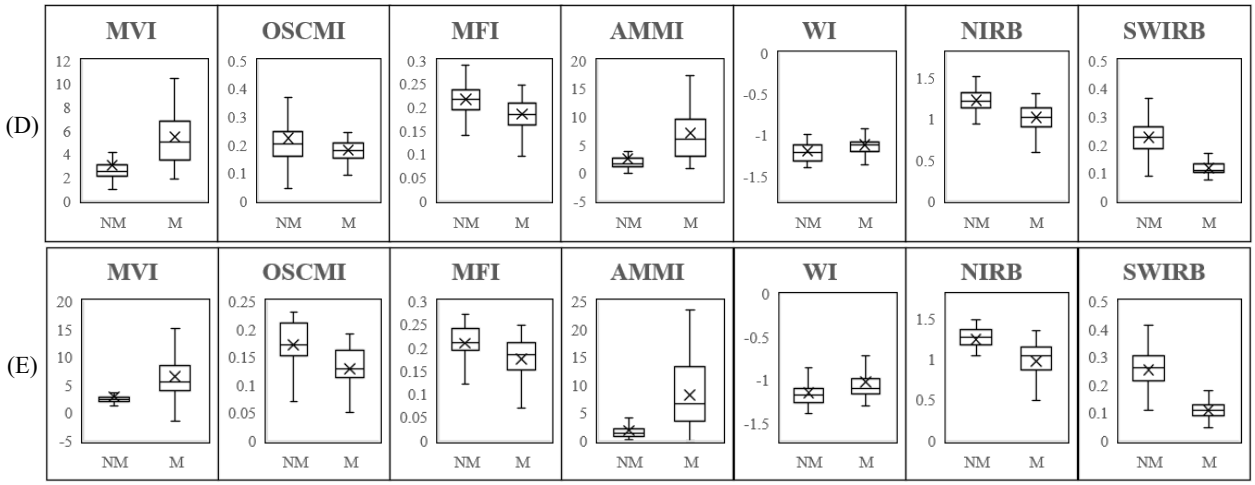

Figure 4. Box plots of the mangrove indices’ values from the validation data for each study area. (A) Puerto Princesa City, Palawan, Philippines; (B) Busuanga, Palawan, Philippines; (C) Siargao Island, Surigao del Norte, Philippines; (D) Select municipalities of Tawi-Tawi, Philippines; (E) Karimunjawa-Kemujan Islands, Indonesia. NM = Non-Mangrove, M = Mangrove.

Mangrove Extent Extraction Index	Optimal Mangrove Threshold	Recommended Mangrove Threshold
MVI	M > [2.7, 5.0]	M > 4.5
OSCMI	M < [0.055, 0.55]	M < [0.04, 0.07]
MFI	M > [0.15, 0.25]	n/a
AMMI	M > [2.0, 5.0]	M > [5.0, 10.0]
WI	M > [-1.25, -1]	M > [-0.50, -0.30]
NIRB	M < [1.13, 1.30]	M < [0.95, 1.10]
SWIRB	M < [0.15, 0.21]	M < [0.15, 0.20]

Table 3. The optimal mangrove threshold of each mangrove index vs the recommended threshold by the proponents.

Neri et al. (2021) concluded that the MVI optimal threshold varies by land cover classes, climatic conditions, or tidal conditions. Mangrove health may also be an additional factor to lower thresholds for MVI (Baloloy et al., 2020; Martinez et al., 2022). The same reasons may apply to the other indices, but further testing of the other indices with smaller areas such as aquaculture lands, irrigated croplands, and sites with palm trees, may provide more insights. It is also possible that the high variation of the optimal threshold is caused by the accumulation of the individual variability of the reflectance bands.

Area (A)	MVI (M > 2.7)		OSCMI (M < 0.24)		MFI (M > 0.16)		AMMI (M > 2.0)		WI (M > -1.15)		NIRB (M < 1.15)		SWIRB (M < 0.21)	
Metric	NM	M	NM	M	NM	M	NM	M	NM	M	NM	M	NM	M
UA (%)	**90.91**	**82.14**	78.94	67.74	60.87	53.25	**84.00**	**84.00**	71.05	62.90	60.00	68.57	**95.45**	**85.71**
PA (%)	**80.00**	**92.00**	60.00	**84.00**	28.00	**82.00**	**84.00**	**84.00**	54.00	78.00	78.00	48.00	**84.00**	**96.00**
OA (%)	**86**		72.00		55.00		**84.00**		66.00		63.00		**90.00**	
κ	0.72		0.44		0.1		0.68		0.26		0.26		0.80	
Area (B)	MVI (M > 2.9)		OSCMI (M < 0.055)		MFI (M > 0.15)		AMMI (M > 2.0)		WI (M > -1.25)		NIRB (M < 1.4)		SWIRB (M < 0.16)	
Metric	NM	M	NM	M	NM	M	NM	M	NM	M	NM	M	NM	M
UA (%)	**90.00**	**90.00**	66.07	70.45	53.57	51.39	**91.49**	**86.79**	71.43	65.52	63.16	58.06	**88.68**	**93.62**
PA (%)	**90.00**	**90.00**	74.00	62.00	30.00	74.00	**86.00**	**92.00**	60.00	76.00	48.00	72.00	**94.00**	**88.00**
OA (%)	**90.00**		68.00		52.00		**89.00**		68.00		60.00		**91.00**	
κ	0.8		0.24		0.04		0.78		0.36		0.20		0.82	
Area (C)	MVI (M > 5.0)		OSCMI (M < 0.55)		MFI (M > 0.25)		AMMI (M > 5.0)		WI (M > -1.00)		NIRB (M < 1.3)		SWIRB (M < 0.20)	
Metric	NM	M	NM	M	NM	M	NM	M	NM	M	NM	M	NM	
UA (%)	78.57	78.57	72.55	73.47	53.23	55.26	78.57	**86.36**	63.63	76.47	61.40	65.12	**94.74**	77.42
PA (%)	**88.00**	76.00	74.00	72.00	66.00	42.00	**88.00**	76.00	**84.00**	52.00	70.00	56.00	72.00	**96.00**
OA (%)	**82.00**		74.00		54.00		**82.00**		68.00		63.00		**84.00**	
κ	0.64		0.48		0.08		0.64		0.36		0.26		0.68	
Area (D)	MVI (M > 3.5)		OSCMI (M < 0.22)		MFI (M > 0.20)		AMMI (M > 3.3)		WI (M > -1.15)		NIRB (M < 1.15)		SWIRB (M < 0.15)	
Metric	NM	M	NM	M	NM	M	NM	M	NM	M	NM	M	NM	M
UA (%)	**80.39**	**81.63**	**83.33**	60.53	45.90	45.10	78.18	**84.44**	61.36	58.93	70	63.33	**93.02**	**82.46**
PA (%)	**82.00**	**80.00**	40.00	**92.00**	44.00	46.00	**86.00**	76.00	54.00	66.00	56.00	76.00	**80.00**	**94.00**
OA (%)	**81.00**		66.00		45.00		**81.00**		67.00		66.00		**87.00**	
κ	0.62		0.32		-0.10		0.62		0.20		0.32		0.74	
Area (E)	MVI (M > 3.3)		OSCMI (M < 0.15)		MFI (M > 0.22)		AMMI (M > 2.5)		WI (M > -1.17)		NIRB (M < 1.13)		SWIRB (M < 0.20)	
Metric	NM	M	NM	M	NM	M	NM	M	NM	M	NM	M	NM	M
UA (%)	**87.04**	**93.48**	59.65	62.79	70.97	59.42	**88.68**	**93.62**	71.43.	70.59	75.86	**85.71**	**97.92**	**94.23**
PA (%)	**94.00**	**86.00**	68.00	54.00	44.00	**82.00**	**94.00**	**88.00**	70.00	72.00	**88.00**	72.00	**94.00**	**98.00**
OA (%)	**90.00**		61.00		63.00		**91.00**		71.00		**80.00**		**96.00**	
κ	0.80		0.22		0.26		0.82		0.42		0.6		0.92	

Table 4. Accuracy assessment of mangrove extraction results using the indices with their respective mangrove extracting threshold. (A) Puerto Princesa City, Palawan, Philippines; (B) Busuanga, Palawan, Philippines; (C) Siargao Island, Surigao del Norte, Philippines; (D) Select municipalities of Tawi-Tawi, Philippines; (E) Karimunjawa-Kemujan Islands, Indonesia. Producer’s Accuracy (PA), User’s Accuracy (UA), Overall Accuracy (OA), Kappa coefficient (κ), Non-Mangrove (NM), Mangrove (M)

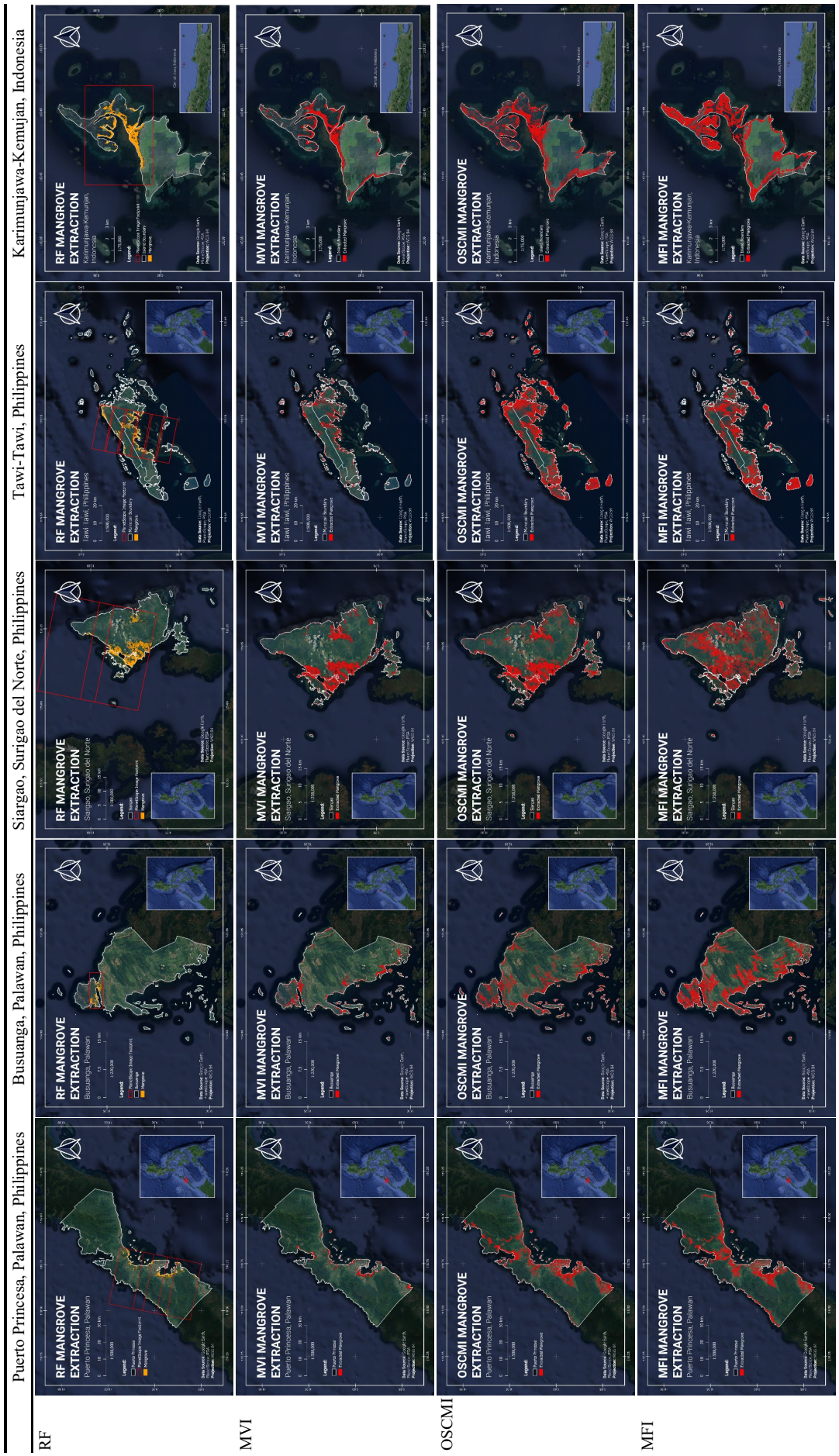
Puerto Princesa, Palawan, Philippines
Busuanga, Palawan, Philippines
Siargao, Surigao del Norte, Philippines
Tawi-Tawi, Philippines
Karimunjawa-Kemujan, Indonesia
RF
MVI
OSCMI
MFI
RF MANGROVE EXTRACTION
MVI MANGROVE EXTRACTION
OSCMI MANGROVE EXTRACTION
MFI MANGROVE EXTRACTION

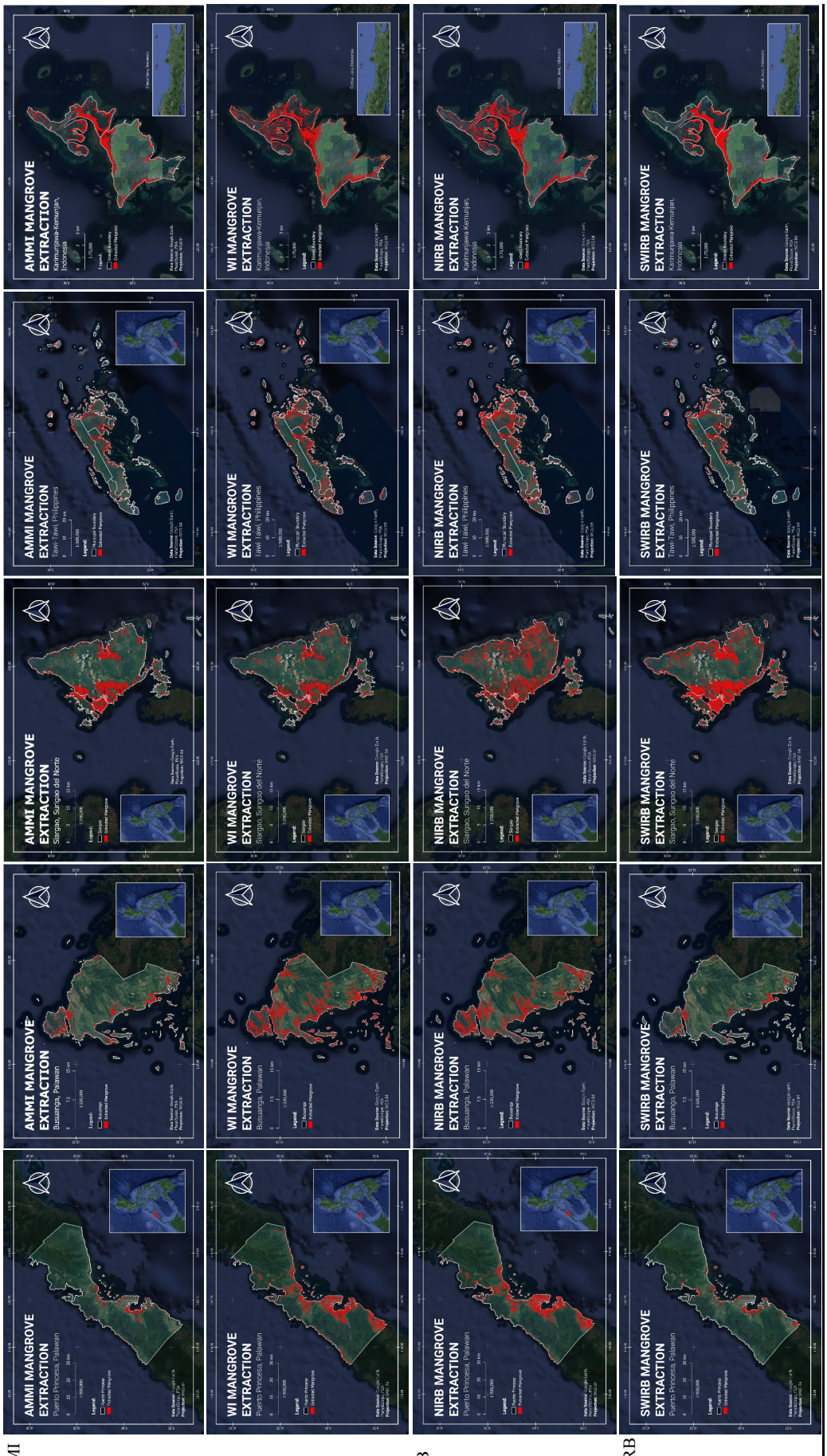

Table 5. Mangrove maps produced from Random Forest classification and selected threshold segmentation-based mangrove extracting indices. The RF output was used for validation of raw extracted mangrove extents of each study area using the indices.

Table 4 shows that only MVI, AMMI, and SWIRB produced consistently high OA that is greater than 80%, even 90% in certain study areas. The three indices did not produce many false positives or false negatives with a consistently high UA and PA.By Landis and Koch's (1977) standards, the κ values of MVI, AMMI, and SWIRB have substantial to an almost perfect agreement with the reference data. These confirm great separability between the two classes from the box plots. Meanwhile, the other indices failed to get an OA of 80% in all study areas. It is notable that MFI got the lowest accuracies and poor κ, indicating that the index is not for mangrove extraction from vegetation pixels. A κ of 0 indicates that the classification agrees with actual data by random chance (McHugh, 2012).

Table 5 shows maps of the mangrove extraction results using RF, and the six (6) threshold segmentation-based indices. The RF results were used for validation and accuracy assessment. By visual inspection, MVI, AMMI, SWIRB performed well in all study areas, showing similar extents to the RF map. OSCMI and WI performed visually well only in Siargao as expected from their box plots in Figure 4, which showed almost separate box values. The rest of the threshold segmentation-based index extraction results are noisy and may have overperformed or underperformed.

The McNemar tests in Table 6 show that MVI, SWIRB, and AMMI mostly have insignificant differences from each other but are significantly different from the other index extraction results. Meanwhile, the other indices have statistically significant differences in certain areas. The consistency of the accuracy without significant differences between the three indices' results implies that the two provide the best mangrove extraction results.

Index Pairs		A	B	C	D	E
MVI	OSCMI	**0.008**	**0.000**	**0.013**	**0.014**	**0.000**
	MFI	**0.000**	**0.000**	**0.000**	**0.000**	**0.000**
	AMMI	0.414	0.655	1.000	1.000	0.317
	NIRB	**0.001**	**0.000**	**0.002**	**0.016**	0.059
	SWIRB	0.102	0.763	0.637	0.134	**0.034**
	WI	**0.000**	**0.000**	**0.004**	**0.000**	**0.001**
OSCMI	MFI	**0.022**	0.063	**0.001**	**0.009**	0.763
	AMMI	**0.040**	**0.000**	**0.029**	**0.022**	**0.000**
	NIRB	0.117	0.182	0.105	1.000	**0.001**
	SWIRB	**0.000**	**0.000**	**0.028**	**0.000**	**0.000**
	WI	**0.014**	1.000	0.197	0.221	**0.025**
MFI	AMMI	**0.000**	**0.000**	**0.000**	**0.000**	**0.000**
	NIRB	0.365	0.317	0.122	**0.023**	**0.001**
	SWIRB	**0.000**	**0.000**	**0.000**	**0.000**	**0.000**
	WI	0.152	**0.046**	**0.012**	0.071	0.170
AMMI	NIRB	**0.002**	**0.000**	**0.004**	**0.022**	**0.034**
	SWIRB	0.083	0.527	0.637	0.157	0.059
	WI	**0.004**	**0.000**	**0.008**	**0.001**	**0.000**
NIRB	SWIRB	**0.000**	**0.000**	**0.001**	**0.000**	**0.000**
	WI	0.622	0.194	0.384	0.289	0.061
SWIRB	WI	**0.000**	**0.000**	**0.008**	**0.000**	**0.000**

Table 6. McNemar Test p-values between all index pairs. Bold values signify significantly different extraction results (at $p < 0.05$). (A) Puerto Princesa City, Palawan, Philippines; (B) Busuanga, Palawan, Philippines; (C) Siargao Island, Surigao del Norte, Philippines; (D) Select municipalities of Tawi-Tawi, Philippines; (E) Karimunjawa-Kemujan Islands, Indonesia

4. CONCLUSION

With the alarming deforestation of mangroves comes the need for rapid and accurate mangrove mapping. Researchers have developed methodologies to aid in this enterprise. One promising method is the use of threshold segmentation-based mangrove mapping indices that uses only a simple formula to extract mangroves from images. The most recently developed ones are the Automatic Mangrove Map and Index (AMMI) by Suyarso (2022) and the Optical and SAR images Combined Mangrove Index (OSCMI) by Huang et al. (2022). The OSCMI proponents claimed their index as the superior mangrove mapping index when compared to its subindices WI, NIRB, and SWIRB, and another threshold segmentation-based mangrove mapping index, the Mangrove Vegetation Index (MVI) by Baloloy et al. (2020). However, the results of this study were found to be the opposite of the findings of Huang et al. (2022).

This study assessed the different threshold segmentation-based indices using Sentinel imagery in five (5) study areas. The researchers used principal component analysis (PCA) as a training guide and Random Forest (RF) Machine Learning algorithm as the classifier on PlanetScope Imagery. Other than OSCMI, its subindices, and MVI, the Automatic Mangrove Map and Index (AMMI) by Suyarso (2022) and Mangrove Forest Index (MFI) by Jia et al. (2018) were included in the assessment. MVI, AMMI, and SWIRB showed consistently high accuracy (greater than 80%) in all study areas. The other indices struggled in separating mangroves from non-mangroves. Furthermore, the results show that threshold segmentation-based indices produce similar results to machine-learning mangrove extraction.

Using the McNemar test, MVI, SWIRB, and AMMI produced insignificant differences from their results but significant differences are found when paired with other indices, proving further their superiority. These three indices only used Sentinel-2 optical imagery. The results refute the postulations of Huang et al. (2022) that the introduction and fusion of SAR imagery (specifically, the VV polarization mode from Sentinel-1) with Sentinel-2 imagery improve mangrove extraction accuracy and the mode is a necessity for mangrove mapping.

The findings were expected from the box plot analysis as only MVI, SWIRB, and AMMI showed good separability between mangroves and non-mangroves. It is notable that box plot results were opposite to that of Huang et al. (2022), with MVI showing weak separability. Neri et al. (2021) did mention that the threshold for MVI is site-specific as it is variable to the environmental conditions and mangrove health (Baloloy et al., 2020; Martinez et al., 2022). Regardless, MVI still reached accuracies of greater than 80% in Huang et al. (2022) in four study areas in China but its statistical significance is yet to be assessed with the other indices' results for that country.

While the results between MVI, AMMI, and SWIRB are similar, SWIRB produced the most accurate results overall. Still, the McNemar test indicates that three indices will provide satisfactory mangrove extraction results without significant difference. The same can be seen in the maps they produced. However, the simplicity of SWIRB (sum of the Sentinel-2's SWIR Bands) may be slightly preferable to MVI and AMMI. Additionally, the optimized threshold of SWIRB is found to correspond with the proponent's recommendation (0.15 to 0.20) in four (4) out of five (5) study areas. If we include the accurate results of SWIRB having the same optimized threshold range in another four (4) study areas in Huang et al. (2022), this implies that SWIRB is the least variable compared to the other indices whose optimized threshold varies per study area and does not match within the range recommendation of their respective proponents. Regardless, MVI and AMMI have other features other than mangrove extraction. MVI seems to correspond with mangrove health (Baloloy et al., 2020; Martinez et al., 2022) while AMMI provides insights into mangrove canopy density

(Suyarso, 2022). SWIRB is yet to be studied for its correlation with mangrove biophysical parameters.

RECOMMENDATIONS

Neri et al. (2021) mentioned that there were missed mangroves due to the application of a vegetation mask from Sentinel quality scene classification layer (SCL). Huang et al. (2022) used NDVI thresholding to produce a vegetation mask. SCL masking may be faster as there is no need to optimize thresholds, but NDVI may produce significant results. Thus, the researchers recommend analyzing their difference in the results of mangrove mapping.

While the RF machine learning algorithm is found to produce high accuracy results in land cover mapping, the use of ground data as inputs to RF may be more reliable and is recommended.

Lastly, only SWIRB had an optimized threshold within the proponent’s recommendation, showing least variability to site and mangrove conditions. However, the studies that observed these are mostly in Asian countries. The threshold of all indices may differ again in different countries, similar to what MVI experienced in the study areas of Huang et al. (2022) in China.

ACKNOWLEDGEMENT

This research work was conducted under the ‘The Project for Comprehensive Assessment and Conservation of Blue Carbon Ecosystems and their Services in the Coral Triangle (BlueCARES) funded by Japan International Cooperation Agency (JICA) and Japan Science and Technology Agency (JST) under the SATREPS Program and the University of the Philippines Diliman. Additionally, the researchers would like to thank Planet Labs for the provision of PlanetScope imagery for the validation of the results of the study.

REFERENCES

Abdu, H. A. (2019). Classification accuracy and trend assessments of land cover-land use changes from principal components of land satellite images. *International Journal of Remote Sensing*, *40*(4), 1275-1300.

Baloloy, A. B., Blanco, A. C., Ana, R. R. C. S., & Nadaoka, K. (2020). Development and application of a new mangrove vegetation index (MVI) for rapid and accurate mangrove mapping. *ISPRS Journal of Photogrammetry and Remote Sensing*, *166*, 95-117.

Elmahdy, S. I., Ali, T. A., Mohamed, M. M., Howari, F. M., Abouleish, M., & Simonet, D. (2020). Spatiotemporal Mapping and Monitoring of Mangrove Forests Changes From 1990 to 2019 in the Northern Emirates, UAE Using Random Forest, Kernel Logistic Regression and Naive Bayes Tree Models. *Frontiers in Environmental Science*, *8*, 102.

Gandhi, S., & Jones, T. G. (2019). identifying mangrove deforestation hotspots in South Asia, Southeast Asia and Asia-Pacific. *Remote Sensing*, *11*(6), 728.

Goldberg, L., Lagomasino, D., Thomas, N., & Fatoyinbo, T. (2020). Global declines in human-driven mangrove loss. *Global change biology*, 26(10), 5844-5855.

Gorelick, N., Hancher, M., Dixon, M., Ilyushchenko, S., Thau, D., & Moore, R. (2017). Google Earth Engine: Planetary-scale geospatial analysis for everyone. *Remote Sensing of Environment*.

Green, E. P., Clark, C. D., Mumby, P. J., Edwards, A. J., & Ellis, A. C. (1998). Remote sensing techniques for mangrove mapping. *International journal of remote sensing*, *19*(5), 935-956.

Gupta, K., Mukhopadhyay, A., Giri, S., Chanda, A., Majumdar, S. D., Samanta, S., ... & Hazra, S. (2018). An index for discrimination of mangroves from non-mangroves using LANDSAT 8 OLI imagery. *MethodsX*, *5*, 1129-1139.

Huang, K., Yang, G., Yuan, Y., Sun, W., Meng, X., & Ge, Y. (2022). Optical and SAR images Combined Mangrove Index based on multi-feature fusion. *Science of Remote Sensing*, 100040.

Jia, M., Wang, Z., Wang, C., Mao, D., & Zhang, Y. (2019). A new vegetation index to detect periodically submerged Mangrove forest using single-tide sentinel-2 imagery. *Remote Sensing*, *11*(17), 2043.

Kamal, M., Farda, N. M., Jamaluddin, I., Parela, A., Wikantika, K., Prasetyo, L. B., & Irawan, B. (2020, June). A preliminary study on machine learning and google earth engine for mangrove mapping. In *IOP Conference Series: Earth and Environmental Science* (Vol. 500, No. 1, p. 012038). IOP Publishing.

Kumar, T., Mandal, A., Dutta, D., Nagaraja, R., & Dadhwal, V. K. (2019). Discrimination and classification of mangrove forests using EO-1 Hyperion data: A case study of Indian Sundarbans. *Geocarto International*, *34*(4), 415-442.

L3Harris. (n.d.). Principal Components Analysis. Retrieved May 17, 2022, from https://www.l3harrisgeospatial.com/docs/principalcomponentanalysis.html

Landis, J.R., & Koch, G.G. (1977) A One-Way Components of Variance Model for Categorical Data. *Biometrics*, 33, 671-679. https://doi.org/10.2307/2529465

Landis, J.R., & Koch, G.G. (1977) A One-Way Components of Variance Model for Categorical Data. *Biometrics*, 33, 671-679. https://doi.org/10.2307/2529465

McHugh, M. L. (2012). Interrater reliability: the kappa statistic. *Biochemia medica*, *22*(3), 276-282.

Mondal, P., Liu, X., Fatoyinbo, T. E., & Lagomasino, D. (2019). Evaluating combinations of Sentinel-2 data and machine-learning algorithms for mangrove mapping in West Africa. *Remote Sensing*, *11*(24), 2928.

National Oceanic and Atmospheric Administration (2013, June 1). *What is blue carbon?* Retrieved March 31, 2022, from https://oceanservice.noaa.gov/facts/bluecarbon.html

National Oceanic and Atmospheric Administration (2021, March 25). *What is a mangrove forest?* Retrieved May 10, 2022, from https://oceanservice.noaa.gov/facts/mangroves.html

Neri, M. P., Baloloy, A. B., & Blanco, A. C. (2021). Limitation Assessment and Workflow Refinement of the Mangrove Vegetation Index (MVI)-Based Mapping Methodology Using Sentinel-2 Imagery. *The International Archives of*

Photogrammetry, Remote Sensing and Spatial Information Sciences, *46*, 235-242.

Niagara, N., Yusuf, M., & Muhammad, F. (2021). The Characteristics of Mangrove Species Are Based on Water Conditions in Karimunjawa Nasional Park. In *E3S Web of Conferences* (Vol. 317, p. 04034). EDP Sciences.

Olofsson, P., Foody, G. M., Herold, M., Stehman, S. V., Woodcock, C. E., & Wulder, M. A. (2014). Good practices for estimating area and assessing accuracy of land change. *Remote sensing of Environment*, *148*, 42-57.

Pham, T. D., Yokoya, N., Nguyen, T. T. T., Le, N. N., Ha, N. T., Xia, J., ... & Pham, T. D. (2021). Improvement of mangrove soil carbon stocks estimation in North Vietnam using Sentinel-2 data and machine learning approach. *GIScience & Remote Sensing*, *58*(1), 68-87.

Powell, V. (n.d.). *Principal component analysis explained visually*. Explained Visually. Retrieved May 22, 2022, from https://setosa.io/ev/principal-component-analysis/

Raschka, S. (2018). MLxtend: Providing machine learning and data science utilities and extensions to Python’s scientific computing stack. *Journal of open source software*, 3(24), 638.

Shi, T., Liu, J., Hu, Z., Liu, H., Wang, J., & Wu, G. (2016). New spectral metrics for mangrove forest identification. *Remote Sensing Letters*, *7*(9), 885-894.

Suyarso. (2022). AMMI Automatic Mangrove Map and Index: An Analytical Study on Satellite Imageries at Aru Islands, Maluku, Indonesia. *Emerging Challenges in Environment and Earth Science Vol*. 2, 106–130. https://doi.org/10.9734/bpi/ecees/v2/3423E

Toosi, N. B., Soffianian, A. R., Fakheran, S., Pourmanafi, S., Ginzler, C., & Waser, L. T. (2019). Comparing different classification algorithms for monitoring mangrove cover changes in southern Iran. *Global Ecology and Conservation*, *19*, e00662.

Viray-Mendoza, V. (2017, November 22). *Mangrove Forests in the Philippines*. The Maritime Review. Retrieved March 31, 2022, from https://maritimereview.ph/mangrove-forests-in-the-philippines/

Xia, Q., Qin, C. Z., Li, H., Huang, C., Su, F. Z., & Jia, M. M. (2020). Evaluation of submerged mangrove recognition index using multi-tidal remote sensing data. *Ecological Indicators*, *113*, 106196.

Xue, Z., & Qian, S. (2022). Generalized Composite Mangrove Index for Mapping Mangroves Using Sentinel-2 Time Series Data. *IEEE Journal of Selected Topics in Applied Earth Observations and Remote Sensing*.

Zhang, X., & Tian, Q. (2013). A mangrove recognition index for remote sensing of mangrove forest from space. *Current Science (00113891)*, *105*(8).